

---

This is an electronic reprint of the original article.  
This reprint may differ from the original in pagination and typographic detail.

Tenhunen, Tiia Maria; Moslemian, Oldouz; Kammiovirta, Kari; Harlin, Ali; Kääriäinen, Pirjo; Österberg, Monika; Tammelin, Tekla; Orelma, Hannes

## Surface tailoring and design-driven prototyping of fabrics with 3D-printing

*Published in:*  
Materials & Design

*DOI:*  
[10.1016/j.matdes.2017.12.012](https://doi.org/10.1016/j.matdes.2017.12.012)

Published: 01/01/2018

*Document Version*  
Peer-reviewed accepted author manuscript, also known as Final accepted manuscript or Post-print

*Published under the following license:*  
CC BY-NC-ND

*Please cite the original version:*  
Tenhunen, T. M., Moslemian, O., Kammiovirta, K., Harlin, A., Kääriäinen, P., Österberg, M., Tammelin, T., & Orelma, H. (2018). Surface tailoring and design-driven prototyping of fabrics with 3D-printing: An all-cellulose approach. *Materials & Design*, 140, 409-419. <https://doi.org/10.1016/j.matdes.2017.12.012>

---

This material is protected by copyright and other intellectual property rights, and duplication or sale of all or part of any of the repository collections is not permitted, except that material may be duplicated by you for your research use or educational purposes in electronic or print form. You must obtain permission for any other use. Electronic or print copies may not be offered, whether for sale or otherwise to anyone who is not an authorised user.

# Surface tailoring and design-driven prototyping of fabrics with 3D-printing: an all-cellulose approach

*Tiia-Maria Tenhunen<sup>1\*</sup>, Oldouz Moslemian<sup>2</sup>, Kari Kammiovirta<sup>1</sup>, Ali Harlin<sup>1</sup>, Pirjo Kääriäinen<sup>2</sup>, Monika Österberg<sup>3</sup>, Tekla Tammelin<sup>1</sup>, Hannes Orelma<sup>1</sup>*

<sup>1</sup> VTT Technical Research Centre of Finland Ltd, P.O. Box 1000, 02044 VTT, Finland, [tiia-maria.tenhunen@vtt.fi](mailto:tiia-maria.tenhunen@vtt.fi), +358 40 744 78 463

<sup>2</sup> Aalto University School of Arts, Design and Architecture, P.O. Box 31000, 00076 Aalto, Finland

<sup>3</sup> Aalto University School of Chemical Technology, Department of Forest Products Technology, P.O. Box 16300, 00076 Aalto, Finland

## Abstract

In this work, we present a new all-cellulose approach for modifying and functionalizing textiles. The use of 3D-printing and two acetylated cellulose derivatives, rigid cellulose acetate (CA) and flexible acetoxypopyl cellulose (APC), on cellulosic fabrics were studied. In addition, prototypes were generated using a design-driven approach. The interactions of cellulose derivatives with cellulose were assessed by quartz crystal microbalance with dissipation monitoring (QCM-D). 3D-printing of cellulosic materials on cellulosic fabrics was performed using a direct-write method by printing cellulose derivatives on woven and knitted cotton and woven viscose fabrics. The adhesion of the printed structures was evaluated via peeling and washability tests. The results indicated that although both cellulose derivatives had a positive attraction towards the cellulose substrate, CA had higher affinity and good adhesion properties, whereas the more branched molecular structure of APC was less firmly attached to cellulosic material. The applicability of 3D-printing cellulosic materials for textile modification and functionalization was assessed through iterative prototyping. Visual effects and functional surface structures were demonstrated. Utilization of 3D-printing of cellulosic materials for surface tailoring of cellulosic textiles, eliminates labour intensive processing or external glues and may enable new and simple customization processes with minimized material usage.

**Keywords:** 3D-printing, cellulose derivatives, cellulose acetate, acetoxypopyl cellulose, design-driven, prototyping

# 1 Introduction

Investigation and development of biobased materials has increased extensively due to the awareness of ecological issues related to traditional petroleum-based polymers [1,2]. New additive manufacturing technologies present high potential for processing these biomaterials. 3D-printing technology, which falls under the vast group of additive manufacturing methods, has an immense potential for developing new application areas in manufacturing industries, but is currently only implemented in incremental number of practical applications [3]. 3D-printing could enable mass customization of products on-demand and in-store by minimizing the material usage [4]. Currently, the most prominent interest in developing 3D-printable biomaterials has been in medical applications, due to their high value potential and demand for biocompatibility [5–7]. However, the increased use of biomaterials could be beneficial in various industries such as textiles and fashion. The substantial utilization of petroleum based materials in textile productions, as well as the add-ons on garments and footwear such as buttons, prints, and labelling in fashion, impede the recycling processes [8]. Cellulose, as the most abundant biopolymer in the world that is fully renewable, non-toxic, and encompasses extremely versatile properties, could be a suitable candidate for replacing these polymeric materials in textiles. Also, due to the high internal affinity of cellulosic materials, by using cellulosic fabrics such as cotton or viscose, the structural bonding could form in the interface without glues or additives that further facilitates the all-cellulose approach [9]. Printable cellulosic materials have the potential to be utilized as printed structuring and topographical modifications, enabling printing of functionalities such as stimuli-responsive materials.

In textile applications, 3D-printing technology is mostly used for creating textile-based structures [10], and in some cases for post-surface modifications using fused deposition modelling (FDM) with thermoplastic polymers (ABS, PLA and Nylon) [11–13]. Although FDM is suitable for many applications, there exist issues surrounding the thermoplastics processing and the narrow selection of materials that are pre-moulded into filaments. Paste extrusion (direct-write or direct ink writing) is a widely used method in biomedical or ceramic applications that utilize paste or gel-like materials [14,15]. Drying or solidifying of the printed material is usually based on evaporation. Direct-write could also be used with cellulosic materials that do not possess the thermoplastic properties required in the FDM method [16]. Moreover, paste extrusions techniques could be adopted for simple post modifications made in shops or at the point of sale [17].

Despite the interest in developing new biomaterials for 3D-printing, limited literature surrounding the 3D-printing of cellulose based materials exists. The previous reports include studies on cellulose dissolved in an ionic liquid and nanocellulose based ink for biomedical applications [18,19]. Printing of cellulosic objects using cellulose acetate and cellulose nanofibrils have also been recently reported [19,20]. Moreover, research on using wood chips with gypsum as a binder to manufacture 3D objects has been conducted [21]. The printing materials chosen for the study were cellulose derivatives with different properties. Cellulose acetate, which is commercially available and widely used, and acetoxypopyl cellulose (APC), which was synthesized from

hydroxypropyl cellulose (HPC) by acetylation. APC has been previously studied mainly due to its ability to form cholesteric liquid crystalline solutions [22,23]. CA and APC materials are chemically similar as both are acetylated, but due to the more branched structure of APC, a difference in material and adhesion properties was expected. 100 % APC forms flexible (amorphous solid) structures and the more linear structure of CA led to the formation of rigid structures.

The key factor in new 3D-printed textile applications is the compatibility of the printed material, the fabric and the 3D-printing system, which requires comprehensive research into existing and new materials, polymer-textile adhesion, and deposition techniques [13]. However, successful utilization of the system requires a multidisciplinary approach in which the possible end-users are taken into consideration. Fusing the disciplines of science and design, this integrative and experimental approach would allow for further strategic realization of prospective trends, contexts of use, and consumer needs, which results in higher impact generation in research [24,25]. Modification and customization of textiles using 3D-printing with bio-based materials could lead to the establishment of new application areas and generate novel design and business concepts.

The aim of this work was to study direct-write 3D-printing of cellulosic materials on cellulosic fabrics and to investigate potential end-use design applications through textile modification and functionalization. Material compatibility of two acetylated cellulose derivatives (CA and APC) on three cellulosic fabrics (woven cotton, knitted cotton, woven viscose) was examined in detail. Interactions between cellulosic materials were studied via adsorption test using quartz crystal microbalance with dissipation monitoring (QCM-D), and via adhesion experiments using peeling and washability tests. The investigation into the versatility of cellulose derivatives in 3D-printing and their suitability for functional textile applications was carried out through experimental and explorative design research approaches [26,27]. Several prototypes were generated by utilizing the experimental findings, portraying the potential end-use design applications and future material development possibilities. Therefore, this work is of high importance in contributing to the generation of new knowledge in the field of utilizing bio-based materials in 3D-printing, while providing valuable trajectories in product design by combining 3D-printing and textiles through functional (rigid and flexible structuring, refractive, thermoresponsive) and decorative (smocking), end-use applications.

## **2 Materials and Methods**

### **2.1 Materials**

**Cellulose fabrics** (Figure 1) used in the 3D-printing studies were uncoated and undyed woven cotton (plain weave, 100% cotton, 150 g/m<sup>2</sup>, Iisalmen kangastukku, Finland), knitted cotton (single knit, 100% cotton, 155 g/m<sup>2</sup>, Orneule, Finland,) and woven viscose (Bamboo Plain Ivory (BB12), 100% viscose, 140 g/m<sup>2</sup>, Whaleys Bradford Ltd., UK). The woven cotton fabric was relatively stiff and had a rough feel, whereas the stretchy knitted cotton was softer (evaluated by hand). The woven viscose fabric was soft and smooth without clear

stretching. Knit textiles are stretchy since they are produced by looping yarns continuously in rows. Woven fabrics are tighter due to multiple yarns that are interlaced at right angles during the production [11]. Chemical composition of the fabrics was investigated with Fourier Transform Infrared spectroscopy (FTIR). The fabrics exhibited cellulosic structure that can be observed from the FTIR spectra typical for cellulose I (cotton) and II (viscose) (Figure S1, supporting information). The measured FTIR peak patterns were comparable to the data reported earlier for regenerated cellulose and cotton [28,29]. Altogether, we can conclude that the fabrics used in the study had highly cellulosic internal structures.

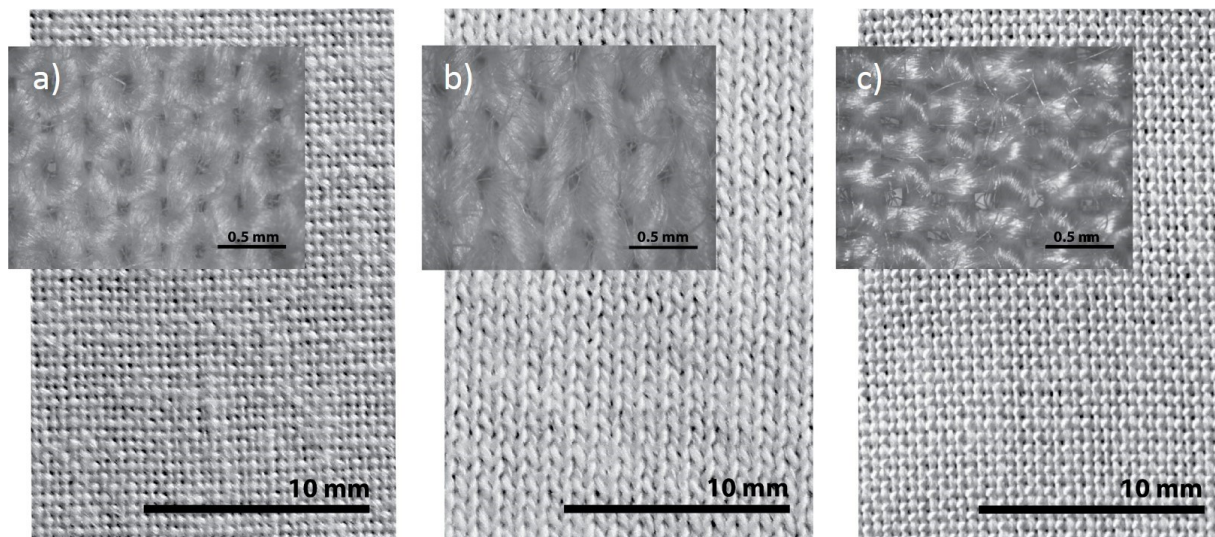


Figure 1 *Photographs of cellulose fabrics used as the substrates for printed structures. a) woven cotton, b) knitted cotton and c) woven viscose fabric. Inserts show microscopy images of the yarn looping of the textiles used.*

**Cellulose derivatives** used in this study were cellulose acetate (CA,  $DS_{Ac}$  of 3,  $M_w \sim 60000$ ) (Figure 2a) and hydroxypropyl cellulose (HPC80,  $DS_{HP}$  of 4-5,  $M_w \sim 80000$ , average  $M_n \sim 10000$ , powder, 20 mesh particle size) (Figure 2b), both obtained from Sigma Aldrich (USA). Trimethylsilyl cellulose (TMSC), used in adsorption investigations, was produced from high purity cellulose powder from spruce (Sigma Aldrich, USA) and synthesized by using a previously reported method [30]. Chemicals used in the synthesis of APC (*N,N*-dimethylacetamide, pyridine and acetic anhydride) were obtained from Sigma Aldrich (USA).

**The QCM-D sensor crystals** were Au coated-crystals (GSX301, from Q-Sense, Gothenburg, Sweden) with a fundamental resonance frequency of ( $f_0$ ) 5 MHz and a sensitivity constant of  $C \approx 0.177 \text{ mg m}^{-2} \text{ Hz}^{-1}$ .

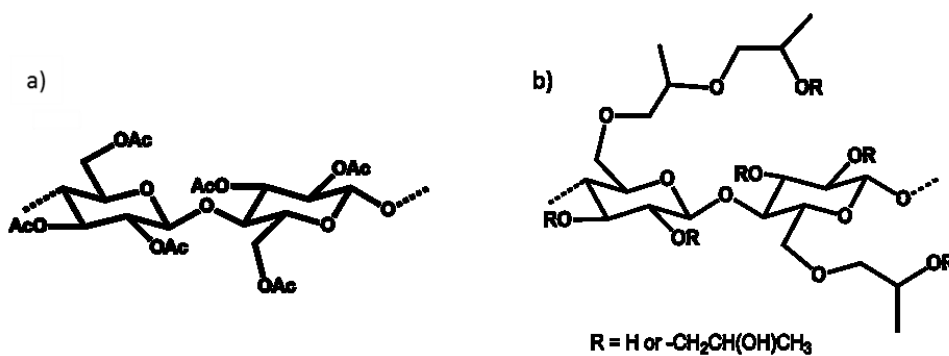


Figure 2 Chemical structures of a) cellulose acetate and b) hydroxypropyl cellulose.

**Prototype materials** for tailoring fabric surfaces were cellulose dissolved in ionic liquid (IL), 1-ethyl-3-methylimidazolium acetate ([EMIM][OAc]), which was obtained from IoLiTec (Germany) and cellulose cotton linters from Milouban (Israel). Thermo-chromic pigment paste used in the prototypes was a commercial product that was acquired from Zenit (Sweden). Reflective beads (commercial high index standard beads, particle size of 180-600 microns, white/clear) were obtained from Cole Safety International (USA). The black colourant used was a commercial food grade paste colourant. Conductive yarn was BEKAERT's Bekinox VN12/1\*275/100Z steel yarn (Belgium). Water used in this study was MilliQ-water. All other chemicals used were analytical grade.

## 2.2 Methods

### 2.2.1 Synthesis of acetoxypropyl cellulose (APC)

Synthesis of APC from HPC via esterification was conducted as described by Tseng et al. [22], with slight modifications. 100 g of HPC (0.62 mol) was first dissolved in *N,N*-dimethylacetamide (HPC consistency of 25 %) at 35 °C. The acetylation was performed by adding 100 ml of pyridine and 100 ml (1.23 mol) of acetic anhydride to the reaction medium (Figure 3). The solution was then allowed to react under stirring overnight at 35 °C and precipitated with deionized water. The precipitated APC was collected and further purified twice with acetone dissolution and water precipitation cycles. The prepared APC was finally dried in a vacuum oven at 40 °C and stored at room temperature until use.

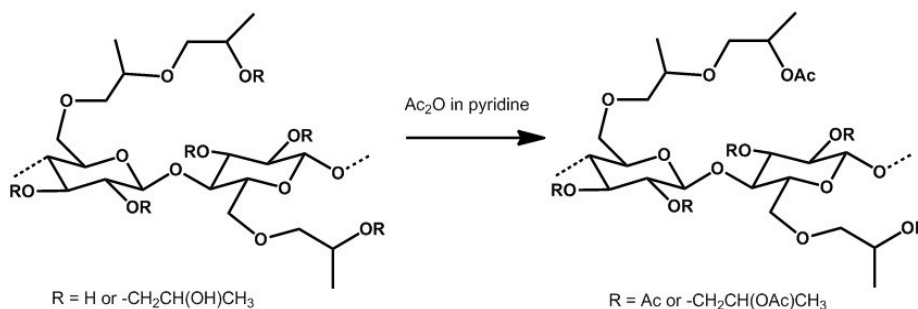


Figure 3 Acetylation of hydroxypropyl cellulose with pyridine and acetic anhydride to acetoxypropyl cellulose

### 2.2.2 Characterization of materials

A **Fourier Transform Infrared Spectroscopy (FTIR)** spectrometer with ATR diamond (Thermo Scientific™ Nicolet™ iS™50 FTIR Spectrometer, United States) was used to determine the chemical composition of the fabrics, synthesized APC, and the purity of the regenerated cellulose from ionic liquid. All spectra were obtained from 32 scans with a resolution of 4 cm<sup>-1</sup> in transmission mode from 350 to 4000 cm<sup>-1</sup>.

A **Liquid state <sup>13</sup>C Nuclear Magnetic Resonance (NMR) spectrometer** (Bruker Avance III 500, Germany) was used to characterize synthesized APC by determining the molar substitution of hydroxypropyl cellulose (HPC) and the degree of acetylation of HPC. APC was dissolved in acetone-d<sub>6</sub> with a concentration of 100 mg ml<sup>-1</sup> and 8 mg ml<sup>-1</sup> and Cr(acac)<sub>3</sub> was added for enhanced relaxation. A BB(F)O double resonance probe head was used at 22 °C to acquire a <sup>13</sup>C spectrum. 20 000 scans were collected with a 1.5 s relaxation delay. Referencing was carried out using the lock frequency, and the spectrum was processed using Bruker TopSpin 3.5 software.

A **Differential Scanning Calorimeter (DSC)**, Mettler Toledo Differential Scanning Calorimeter model DSC2 (Mettler Toledo GmbH, Switzerland), was used to characterize synthesized APC by determining the glass transition temperature. The DSC measures the temperature and heat flow associated with the thermal transition of a material. The calorimeter was equipped with an intra-cooler (TC100MT, Huber, Germany) allowing a minimum starting temperature of -90 °C. N<sub>2</sub> flow used was 80 ml min<sup>-1</sup> in order to purge the measurement cell and prevent water condensation. For the measurement, 40 µl sealed aluminium crucibles were used.

### 2.2.3 Assessment of the interactions via adsorption investigations using QCM-D

A Quartz crystal microbalance with dissipation monitoring (QCM-D E4, Q-sense AB, Gothenburg, Sweden) was used to investigate the adsorption of CA and APC on a pure cellulose surface. The QCM-D technique is an acoustic method that is sensitive to the mass changes on the crystal surface [31,32]. The QCM-D technique simultaneously measures the frequency and dissipation changes on the crystal surface at a fundamental resonance frequency and its overtones. The piezoelectric quartz crystal oscillates at a resonance frequency,  $f_0$ . Frequency depends on the total oscillating mass (including the solvent) and it increases or decreases with mass changes on the crystal surface. The amount of adsorbed material can be calculated using the Sauerbrey equation [33] if the mass of adsorbed materials is evenly distributed, rigid and small (compared to the mass of the crystal). In this case, the shift in frequency  $\Delta f = f - f_0$  is related to the adsorbed mass,  $\Delta m$ , per unit surface.

$$\Delta m = -\frac{c\Delta f}{n} \quad (2)$$

where  $C$  is a constant that describes the sensitivity of the device to changes in mass and  $n$  is the overtone number ( $n = 1, 3, 5, 7$ ). When the material is coated onto a crystal surface, the adsorption of studied material onto substrate can be monitored on-line [34].

If the film on the sensor surface is not fully elastic or rigidly attached, frictional losses occur that lead to damping of oscillation with a decay rate of amplitude, which is dependent on the viscoelastic properties of the material. The change in dissipation ( $\Delta D = D - D_0$ ) measures qualitatively the softness and rigidity of the film on the sensor surface and is calculated using dissipation,  $D$ , defined by Eq. (1).

$$D = \frac{E_{diss}}{2\pi E_{stor}} \quad (1)$$

where  $E_{diss}$  is the total dissipated energy during one oscillation cycle and  $E_{stor}$  is the total energy stored in oscillation. The film can be considered fully elastic and rigid when  $\Delta D \leq 1 \times 10^{-1}$ , and there is no spreading of the overtones.

Prior to the QCM-D measurements, the bare crystal surfaces were deposited with TMSC using a spin coating procedure and regenerated to cellulose [35]. The gold coated QCM-D crystals were first cleaned by UV/ozone treatment for 30 min. Subsequently, the crystal was wetted with toluene, following spinning at a speed of 3000 rpm for 15 s to purify the crystal surface. 10 mg ml<sup>-1</sup> of TMSC in toluene was then spin coated onto the crystal surface with a speed of 4000 rpm for 60 s. Finally, the coated crystals were dried in an oven (60 °C) for at least 10 min to ensure sufficient adhesion. Desilylation was carried out in 10 % HCl vapour in vacuum for 5 minutes. After regeneration of TMSC to cellulose, the cellulose surfaces were kept in MilliQ-water overnight before conducting the measurements with the QCM-D. Just before the measurement, the cellulose surfaces were gently dried with nitrogen gas and placed in the QCM-D chamber. Acetone was pumped through the chamber until a plateau frequency signal was achieved. Then, CA or APC dissolved into acetone was allowed to flow over the cellulose surface. Acetone was used as a solvent for both materials, due to the hazardous nature and distinctive smell of 100% acetic acid, which would have been difficult to remove and could have damaged the sensitive system. Adsorption studies were performed with dilute dispersions (0.5 mg ml<sup>-1</sup>) in acetone at a flow rate of 0.1 ml min<sup>-1</sup> with a constant temperature of 22 °C. All measurements were replicated twice.

#### **2.2.4 Preparation of printing pastes**

The printable CA solution was prepared by dissolving commercial CA in acetic acid (concentration 30 w-%). The APC solution was produced by dissolving APC in acetone in a concentration of 80 w-% using rotating vials.

For prototyping purposes, cellulose cotton linters were dissolved in [emim]OAc in 10% concentration. Dissolution of cotton linters was done in a vertical kneader system following the previously reported procedure [36]. The dissolved cellulose in ionic liquid was stored in a sealed bottle at room temperature prior to 3D-printing.

### 2.2.5 3D-printing of cellulosic materials on fabrics

The modification of fabric surfaces was carried out using a commercial direct-write 3D-printer (3Dn-300, nScript Inc., USA). The 3D-printer system used is based on an extrusion technique for paste-like materials with a wide range of suitable viscosities. The system utilizes a simple syringe pump system with disposable 2.5 ml syringes and tapered tips. The nozzle size of the tip used was 0.84 mm (Nordson EFD, USA). Printing speed used for materials was 5 mm/s. The printing pressure was set at 41.5 psi for CA and at 20.5 psi for APC, due to its lower viscosity. Fabrics were attached onto plastic films using adhesive tape during printing and drying.

Moreover, an in-house built 3D-printer was used for prototyping purposes. This 3D-printer functioned exactly the same way as nScript by utilizing the extrusion technique and tapered tips.

### 2.2.6 Adhesion of printed materials via peeling test

The adhesion of printed structures to cellulose fabrics was investigated utilizing a Lloyd materials testing machine LS5 (Lloyd Instruments Ltd., UK) with a 100 N load cell. The system measures the tensile force as a function of material extension that correlates with the load needed to peel the printed structure from a fabric (Figure 4c). Preload of the experiment was 0.5 N (preload speed 1 mm/min) and the separation speed was kept at a constant of 5 mm/min. All measurements were carried out in standard conditions at 23 °C with 65 % humidity. All samples were stored for 24 hours in standard conditions prior to mechanical testing. Three measurements were taken from each sample point.

Printed structures for the peeling resistance measurements were prepared by printing half of the structure on fabric and the other half of the structure on a tape on the fabric with two successive layers (Figure 4a). The tape prevented adhesion to the fabric, and the other end of the structure could be mounted between jaws of the material tester. The dimension of the test strip was 10 mm × 40 mm and the adhered print on the fabric was 20 mm long.

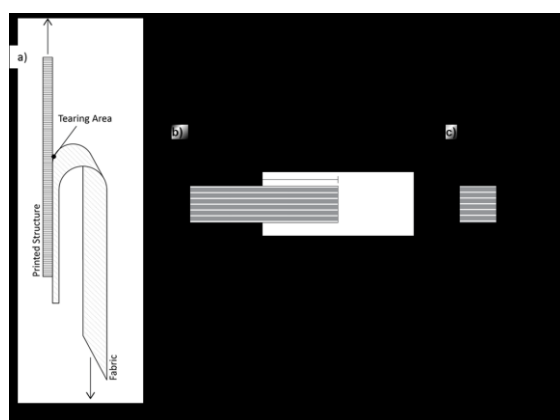


Figure 4 a) Schematic image of peeling test: printed structure and fabric are attached between clamps and pulled apart at an angle of 180° and fabric samples for printed structures for b) peeling resistance and c) washing tests

### 2.2.7 Washability testing of 3D-printed structures

The washability test was utilized to investigate the durability of the printed structures on cellulose fabrics. The test was carried out using standard ISO 6330 (Domestic washing and drying procedures for textile testing) with standard washing powder (IEC-A Reference Detergent 60456 without phosphate) at 40 °C for 48 min. Two layered structures with 10 mm × 10 mm dimensions were printed for washability tests (Figure 4c). The solvents in the printed CA and APC structures were evaporated in vacuum hood conditions. Five washing cycles were conducted and after each wash cycle, the printed structures were dried on a flat surface in air and were observed with both the naked eye and a microscope. The dried structures were evaluated with the following criteria: +++ = no change, ++ = print has peeled-off at its corners, + = only small amount left, - = nothing left.

### 2.2.8 Design-driven prototyping for 3D-printing

Five types of prototypes (refractive, thermoresponsive, rigid structuring, flexible structuring and smocking) were printed using the studied materials, and cellulose dissolved in IL. ACP (pure and coloured) in acetone was used for flexible printed fabric structures and CA in acetic acid for rigid structuring. The refractive printing material was prepared by mixing reflective beads in CA and acetic acid. The thermochromic pigment paste was mixed with the APC dissolved in acetone. The smocking of the fabric was carried out using the ionic liquid dissolved cellulose. The smocking patterns were specifically designed to experiment visual effects and the samples were regenerated in a water bath overnight and dried in air, which caused the formation of the pattern by shrinkage in the fabric. The printed structures were allowed to set for approximately one hour prior to regeneration in a water bath. All mixing was done using a SpeedMixer™ DAC 150 SP (FlackTek Inc., UK).

## 3 Results and discussion

In this work, the potential of utilizing 3D-printable cellulosic materials for surface tailoring and functionalizing cellulosic fabrics was studied. Prior to printing, the prepared materials were characterized and the material interactions were studied via adsorption tests, and after printing, via peeling and washability tests. Finally, the materials were utilized in prototypes.

### 3.1 Characterization of acetoxypopyl cellulose (APC)

Acetoxypopyl cellulose (APC) was synthesized by esterification of hydroxypopyl cellulose (Figure 3). Structural analysis and grafting density of synthesized APC were determined of using FTIR and liquid state <sup>13</sup>C NMR spectroscopy. In FTIR spectra (Figure S2, Supporting information), acetylation of HPC can be observed from the appearance of a C = O ester band at around 1740 cm<sup>-1</sup>, an asymmetric C-O-C stretching peak of an acetate ester centered at 1240 cm<sup>-1</sup>, and the reduction of the wide hydroxyl stretching band in 3200-3700 cm<sup>-1</sup> [22,23]. From quantitative <sup>13</sup>C NMR spectra, the molar substitution of hydroxypopyl cellulose is

determined by the peak area of  $-CH_3$  signals of the hydroxypropyl substituents ( $\sim 15$  ppm) and the degree of substitution for acetylation at the peak area of acetyl substituents ( $\sim 170$  ppm). According to the spectra (Figure S3, supporting information), the molar substitution of hydroxypropyl cellulose was  $MS_{HP}$  4.3 and the degree of substitution for acetylation was  $DS_{Ac}$  3.0, which implies that all free hydroxyl groups were acetylated.

In DSC measurement, a glass transition temperature of  $T_g$   $-8$  °C (Figure S4, Supporting information) was acquired, which is comparable to the previously reported value for APC by Rusig et al. [37].

### 3.2 Interactions of cellulose derivatives with cellulose revealed with QCM-D

In order to elucidate the cellulose-cellulose derivative interactions and to further understand the processes taking place during 3D-printing, the adsorption studies were carried out on pure cellulose thin films deposited on a QCM-D sensor surface. The compatibility as well as the strength of interactions between either CA or APC with cellulose can be qualitatively monitored by following their time dependent adsorption behaviour. Figure 5a-b shows the change in frequency and the change in dissipation as a function of time for the adsorption experiments of  $0.5 \text{ mg ml}^{-1}$  CA and APC dispersions dissolved in acetone.

Prior to the introduction of the dilute dispersions of either CA or APC, the cellulose surface was allowed to stabilise in acetone for approximately 10 min. After the replacement of acetone in the QCM-D chamber with an acetone solution of cellulose derivative, the adsorption was monitored for 60 min followed by the gentle washing step of the system with pure acetone. As shown by Figure 5a, both cellulose derivatives induced clear negative frequency changes with a simultaneous increase in dissipation factor (Figure 5b) corresponding to a mass increase taking place on the cellulose coated sensor surface. CA instantaneously adsorbs on cellulose yielding a frequency and dissipation change of  $-39$  Hz and  $6.5 \times 10^{-6}$ , respectively. The frequency change of APC was significantly smaller ( $-10$  Hz) with a simultaneously recorded dissipation change of  $3 \times 10^{-6}$ . In addition, in the case of APC, the adsorption equilibrium was not completely reached within 60 min. Gentle acetone washing did not significantly remove either of the adsorbed cellulose derivatives. Minor changes in frequency and dissipation responses indicate that changes in adlayer conformation are more likely than remarkable ongoing desorption. Qualitative interpretation of the QCM-D data suggests that both cellulose derivatives indeed possess a positive attraction towards cellulose. When looking at the rate of adsorption as well as the amount of adsorbed material at the end of the process, it seems that APC was less prone to adsorb on cellulose compared to AC, which indicates its lower affinity towards cellulose. However, the rinsing with pure acetone resulted in only a minor increase in the frequency of oscillation. This indicates either negligible removal of material or reorganization of the adsorbed layer [38], which points towards relatively strongly attached polymers on the cellulose sensor surface.

There were no previous QCM data in the literature for adsorption of CA or APC or for adsorption of materials in acetone on pure cellulose model film. Hence, the adsorption data was compared to changes in frequencies made in water. Previous studies of the adsorption of chitosan on a pure cellulose surface in water reflected a -

9 Hz change in frequency [39] and anionic CMC adsorption on cellulose in water reflected a -40 Hz change in frequency [40]. Therefore, it can be concluded that acetone acts relatively well as an adsorption medium for acetylated cellulose derivatives in a similar fashion to water for water-soluble cellulose derivatives.

In order to compare the viscoelastic properties of the adsorbed layers of cellulose derivatives, the QCM-D data was plotted as change in dissipation versus change in frequency (Figure 5c). This approach allows the determination of the ability of the adsorbed layer to bind energy, i.e. the steeper the  $\Delta D/\Delta f$  curve, the more dissipative the layer is and the more energy is bound per frequency change unit [41]. Both cellulose derivatives display a perfectly linear relationship and the  $\Delta D/\Delta f$  ratio at the end of the adsorption is equal, which suggests that a similar amount of energy is bound and exhibits layers with similar viscoelastic properties. When compared to the linear structure of CA, we can speculate that the branched structure of APC does not have a significant influence on the physical properties of the adsorbed layer. However, CA seems to have higher affinity towards cellulose, as shown in Figure 5a, due to a significantly higher adsorption rate and the absorbed amount of CA compared to APC. In order to attain further clarification on true adhesion after drying, a more detailed analysis of cellulose derivatives on cellulose substrate will be investigated by means of practical peeling and washability tests.

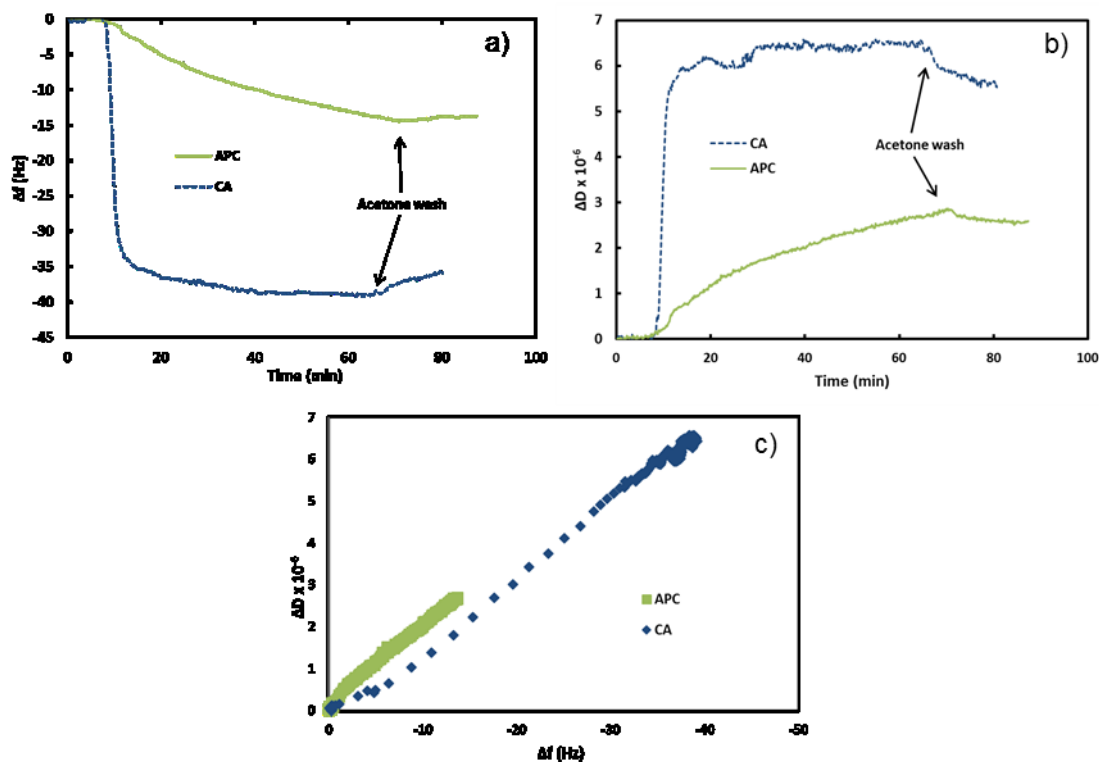


Figure 5 a) The change in the frequency and b) dissipation on the adsorption of dilute CA and APC dispersions on pure cellulose surfaces followed by rinsing with acetone. c) Change in dissipation factor as a function of the change in frequency for adsorption.  $f_0 = 5$  MHz,  $n = 5$

### **3.3 3D-printing of cellulose acetate and acetoxypropyl cellulose**

As CA and APC are soluble in both acetone and acetic acid, these two solvents could be, in principle, used to form printable solutions of the materials suitable for direct-write printing on commercial cellulosic fabrics. Acetone evaporates faster compared to acetic acid. However, for CA, it was observed that the slower evaporation rate was more expedient in 3D-printing. Thus, acetic acid was used as a solvent for CA. This improved the processability, enabled printing of several layers, and prevented clogging of the printer nozzle. The printing was conducted with a 30 w-% of CA content, which was considered a good compromise to achieve the required printing quality. High viscosity or a high solids content is usually desired in direct-write 3D-printing method and results in better 3D-formation and smaller shrinkage. However, if the viscosity is too high the material does not extrude or attach to the substrate. Therefore, the 3D-printing process requires optimization between the printability, shrinkage, and adhesion properties. According to visual observation, the printed CA on the fabric formed a transparent layer and the two successive layers fused evenly together. It was perceived that during solvent evaporation, shrinkage of the printed CA structure caused mild creasing of the fabric consequent of the relatively high solvent content of the printing dope. However, minor shrinkage can be prevented by stretching the textile while drying.

In case of APC, acetone was used as a solvent. The faster evaporation rate of acetone, did not induce similar limitations as in the case of CA, therefore, it seemed more practical choice for solvent. Visually, APC forms a white layer, which after drying, is soft, flexible, and slightly tacky without any fabric shrinkage. It was observed that the 3D-printer could process APC in much higher concentrations (~80 w-%) compared to CA due to the lower viscosity of the material. No significant changes to the quality of the print were noticed between tested fabrics.

### **3.4 Adhesion of the printed structures**

#### **3.4.1 Peeling test**

Adhesion of the fabric and printed material is largely affected by the contact area, which is closely related to material compatibility and the textile structure [11,42]. In order to achieve firm adhesion, the polymer should be compatible with the fabric and penetrate and spread evenly on the yarn surfaces [10]. The adhesion of printed CA and APC on cellulose fabrics was investigated by using a tensile testing approach with the T-peel test. The force required to peel the printed structure off the fabric was measured from a 10 mm wide strip with a separation speed of 5 mm/min, which gave an indication of the mechanical durability of the print when used in textile applications. The results were converted to N/100 mm width by dividing the average load by the width of the specimen and then multiplying by 100 [43]. The average peeling forces are presented in the force-extension curves in Figure 6 and Table 1.

In Figure 6, the first slope in the force-extension curve comprises the physical elongation of the fabric. Thereafter, the peeling of the print from the fabric or tearing of the fabric starts to dominate. It was observed that the type of fabric (woven or knitted) significantly altered the shape of curves, e.g. the knitted fabric stretched significantly more than the woven fabrics (Figure S5, supporting information). Due to the fragility of the viscose fabric, the strength of adhesion of the printed CA structure could not be measured and the result for CA on viscose in Figure 6 and in Table 1 represent the force required to tear the fabric. Therefore, in this case the strength of adhesion overpowered the strength of the fabric. The average peeling forces from three parallel measurements for CA on woven and knitted cotton fabrics were within a similar range. However, CA on knitted cotton required slightly higher peeling strength. This could be due to the more complex structure of the knit in z-direction that enables more surface area for adhesion.

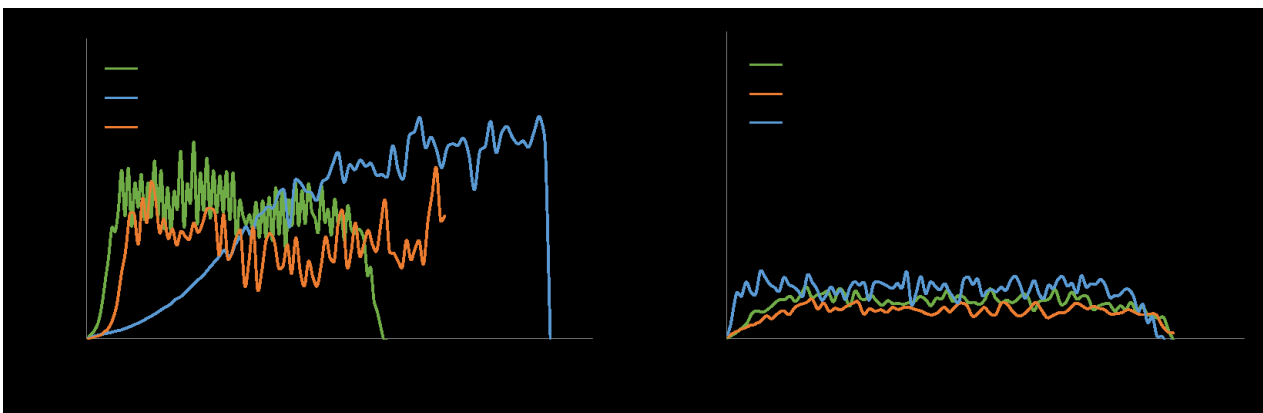


Figure 6 The peeling force as a function of machine extension for CA (left) and the peeling force as a function of machine extension for APC (right) \*fabric tore instead of peeling.

Table 1 Average peeling force converted to N/100 mm width (speed 5mm/min) with standard deviations. 3 parallel measurements. \*viscose fabric tore instead of peeling.

Average peeling force (N/100 mm width)	Woven cotton	Knitted cotton	Woven viscose
CA	124.8 ± 2.0	193.0 ± 19.2	(90.8* ± 1.7)
APC	12.2 ± 1.7	15.1 ± 10.0	15.0 ± 4.3

The maximum peeling forces of APC on all tested fabrics were approximately 1/10 of peeling forces of CA (10-20 N/100 mm versus 150-250 N/100 mm, respectively) (Figure 6b). Significantly less force was needed to peel the printed APC from the surface of the fabric compared to CA. It can be speculated that the longer

substituents of APC lead to the lower adhesion with the cellulose surfaces of the fabrics, which may explain the peeling results. Moreover, the high solids content (80 w-%) and the use of fast drying acetone as a solvent might prevent the material from passing into the fabric structure and lower the contact area between the print and the fabric.

Sanatgar et al. [13] have previously measured the average peeling force values for printed nylon on polyamide (PA) (40-120 N/100 mm width) and for printed polylactic acid (PLA) on PA (5-70 N/100 mm). Due to differences in measurement conditions (25 mm wide testing strip and 100 mm/min peeling rate in their case), the average peeling forces could only be qualitatively compared. In comparison, the average peeling force of CA with tested cotton fabrics can be considered at the very least as high. Whereas, the peeling results of APC suggest a relatively poor adhesion to the tested fabrics. However, in our case, a slower peeling rate that requires less energy to peel was used. Therefore, the values should be in fact greater than those presented in Table 1 [44,45]. It is conceivable that CA is very compatible with the cellulose textile materials and diffused into the fabric structure, increasing the contact area between the print and the fabric.

The adhesion of synthetic FDM 3D-printable polymers (ABS and PLA) on fabrics (polyester, polypropylene, wool, polywool, knit soy and woven cotton) have also been studied by Pei et al. [11]. In their study, woven cotton fabric presented the best results in adhesion properties and good compatibility with non-cellulosic polymers. In general, natural fabrics or natural fabric blends were better suited for 3D-printing purposes.

### **3.4.2 Washability test**

The mechanical durability of printed cellulose structures was investigated with a standard washing test. Samples were washed 5 times with detergent according to standard ISO 6330, which is the most widely used method to determine visible changes in the appearance of the textile after a number of washing cycles [46,47]. Results presented in Table 2 demonstrate how well the textile would last in domestic washing [48]. Printed CA came only slightly off from its corners during the first wash, but endured all 5 washing cycles without significant changes.

APC did not endure any of the washing cycles. As shown in peeling tests, adhesion between APC and cellulose fabrics was significantly lower compared to CA and fabrics. In addition, acetylation of HPC alters the solubility behaviour of the polymer while pure HPC is soluble in cold water when  $MS_{HP}$  is approximately 4 [16,22]. Based on this, it seems that poor adhesion plays the main role, although, the contribution of surface active components of detergents cannot be completely ruled out. The choice of fabric did not affect the results.

The washability results support the interaction and peeling data. 3D-printed CA could be used in textile applications where mechanical durability and wash resistance are needed. Whereas, the strength of the bonding between the APC and fabric requires improvement or alternatively, different types of textile applications should be considered.

Table 2. Washability tests of the CA and APC printed fabrics during five washing cycles.

Sample	Fabric	1. wash	2. wash	3. wash	4. wash	5. wash
CA	Woven cotton	++	++	++	++	++
	Knitted cotton	++	++	++	++	++
	Woven viscose	++	++	++	++	++
APC	Woven cotton	-	n.a.	n.a.	n.a.	n.a.
	Knitted cotton	-	n.a.	n.a.	n.a.	n.a.
	Woven viscose	-	n.a.	n.a.	n.a.	n.a.

- = nothing left

+ = only partially left

++ = print has come off its corners

+++ = no change after washing

### 3.5 Design-driven prototyping - 3D printing of functional and decorative structures

The material and design experimentations described in this section demonstrate the potential of using cellulosic materials in 3D-printing on cellulosic textiles, utilizing the knowledge generated in the first section of the study. In this design-driven development, the integrative and nonlinear design approach provided insight into the identification of potential challenges and opportunities in the utilization of new materials and technologies [49,50]. In this study, the examples were developed through iterative prototyping methods [51], in which the qualities and capacities of the materials were explored. Prototyping is used as a tool to broaden the possibilities of development and to concretize ideas from different angles. Additionally, it enhances communication and understanding through tangible and visual representations [52,53]. Direct-write printing was utilized to study the usability of the materials in textile modifications. In addition to CA and APC, we also demonstrated the utilization of cellulose dissolved in ionic liquid (IL), [emim]OAc.

#### 3.5.1 Functional prototypes

In many textile applications, good adhesion and the ability to wash are crucial properties (e.g. seams). However, there are also applications where these properties are not needed and in some cases, such as disposable textiles, the possibility to remove the material by washing could be advantageous. 3D-printing of

structures or patterns on textiles enables personalization of the material or product. Textiles can be mass manufactured through traditional methods and post-customized by printing according to the intended application or to the individuals' needs. There are several advantages in using wood-based materials for textile modifications. In general, cellulose-based materials are from renewable resources and environmentally safe and are often also hypoallergenic [54,55]. By using chemically similar materials, the post-consumer textile recycling could be simplified.

To validate the usability of cellulosic materials for integration of functionalities onto cellulosic fabrics five types of prototypes were developed (refractive, flexible structuring, rigid structuring, thermoresponsive, and smocking). In refractive prototypes, reflective glass beads were mixed in CA caused the material reflect light and printable reflectors could be produced. This prototype verifies the ability to attach active components on cellulose fabrics by using CA as a binder. The prototypes of flexible structuring were made to demonstrate the 3D-printing of all-cellulosic textiles (Figure 7b-c and Figure 7e-f) using pure and coloured APC. These prototypes showcase application potential for implementation of printed seam materials replacing stitches (Figure 7b, e), printed non-slip structures (Figure 7c), and printed pads for knees or elbows (Figure 7f). The third prototype was rigid structuring that can be used to control the stretch of the textile (Figure 7d). The thermoresponsive prototypes utilized thermochromic powder, mixed into the APC solution, resulting in a printable thermoresponsive cellulose tag (Figure 7g). The same technology can be used for indicator purposes and in Figure 7h a conductive metal yarn was embedded into the print. When current was passed through the wire, the heat produced by the resistance of the wire changed the colour of the printed tag on the fabric. Cellulose acted as an indicator, while providing protection against direct skin contact with the wire.

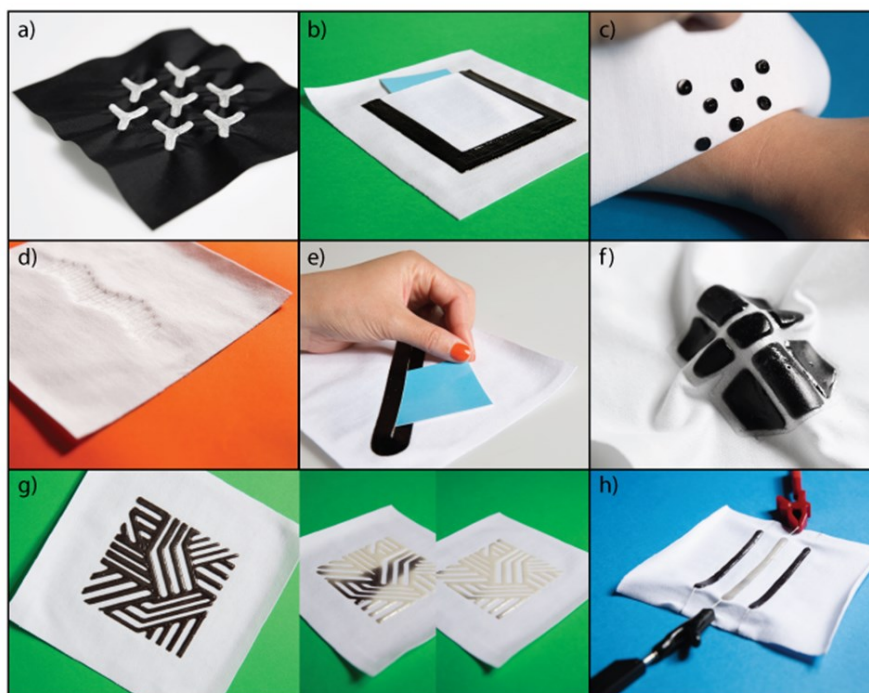


Figure 7 a) Reflective beads mixed with CA to form reflective structures b-c) Structures printed with coloured APC d) CA on a controlled stretch structure e-f) Structures printed with pure and coloured APC g) APC mixed with thermochromic pigment paste to form thermoresponsive structures h) Thermochromic structures with APC (design: Pauliina Varis, photos: Eeva Suorlahti)

### 3.5.2 Decorative prototypes

Ionic liquid (IL) has been previously used in 3D-printing of dissolved cellulose [19] and for partial dissolution of cotton fabric [56]. These approaches led to a hypothesis that ILs could be utilized to permanently bind printed structures to cellulosic fabrics, as the printed IL dissolved cellulose can chemically entangle with the filament surfaces of the fabric via partial surface dissolution [56]. The cellulose content in the IL was 10% and the material itself was very viscous requiring high pressure for extrusion in 3D-printing. During printing, the adjacent lines and layers were completely fused together since the IL dissolved cellulose requires regeneration with water for precipitation into a solid form. The high viscosity of the cellulose solution created challenges for forming sharp corners. Another challenge in this process was to produce high structures, due to the collapse of the printed material before regeneration. Similar behaviour has been reported in previous literature [19]. The cellulose concentration of IL dissolved printing dope could be potentially increased up to 16% in [emim]OAc or even higher if microwave heating is used. [57,58].

Subsequent to printing, the samples were placed in excess water, acting as an anti-solvent, in order to regenerate the cellulose and remove the remaining ionic liquid. After regeneration, the print presented a swollen hydrogel structure (Figure S6, supporting information). It is reported that in thin structures, such as in

filaments, the cellulose coagulation is faster compared to the behaviour in thick structures, as the diffusion to the inner structures is decreased by the dense gel surface [59]. Therefore, the printed structures were kept in water overnight to ensure that all IL was removed from the printed cellulose. This was confirmed by FTIR (Figure S7, supporting information). The hydrogel structures were dried in air, which caused significant shrinking and hardening of the printed material (Figure S6, supporting information). It was observed that the cellulose printed from IL was strongly attached on the fabric.

The strong shrinking property of cellulose dissolved in IL was utilized to induce smocking of the fabric for novel textile design (Figure 8). The smocking effect achieved by the 3D-printing of IL dissolved cellulose makes the structuring process of fabric fast, easy, and affordable. In addition, it can be applied according to need, thus allowing more freedom throughout the design process. The IL structure was also proven (results not shown) to be washable and retained its form.



Figure 8 *Structures printed using cellulose dissolved in ionic liquid could be used for smocking effects (design: Pauliina Varis and Ilona Damski, photos: Eeva Suorlahti)*

## 4 Conclusions

In this paper, a multidisciplinary all-cellulose approach for surface tailoring and functionalizing textiles was presented. We have investigated the use of 3D-printing and two cellulose derivatives, rigid CA and flexible APC, for the modification of cellulosic fabrics. Detailed studies of the adsorption of the cellulose derivatives to cellulose and durability tests were combined with prototyping of 3D-printable cellulosic textile applications

using a design-driven approach. It was determined that due to its more branched molecular structure, APC was less firmly attached to cellulosic materials as indicated by the QCM-D, peel tests, and washing tests. Meanwhile, the linear structure of CA enabled the material to align well with cellulose molecules in the substrate, resulting in good adsorption and excellent adhesion properties for the printed structures. However, both materials could be considered suitable for use in textile applications and the application potentials were successfully presented via different functional and visual textile demonstration models. Utilization of 3D-printing of cellulosic materials on cellulose fabrics opens new perspectives in developing all-cellulose textile customization without labour intensive processing. Moreover, by using renewable and recyclable materials, the development of new products and services could be implemented in an environment friendly fashion.

### ***Acknowledgments;***

This work has been funded by Tekes (Finnish Funding Agency for Innovation) through a strategic opening entitled Design Driven Value Chains in the World of Cellulose 2.0. We acknowledge the contributions of Pauliina Varis and Ilona Damski from Aalto University School of Arts, Design and Architecture for textile designs, Harri Setälä for cellulose derivative chemistry, Arja Puolakka from Tampere University of Technology for the washability tests, and Hanna Iitti (VTT) and Ville Klar (Aalto University) for the 3D-printing.

## **References**

- [1] T. Willke, K.-D. Vorlop, Industrial bioconversion of renewable resources as an alternative to conventional chemistry, *Appl. Microbiol. Biotechnol.* 66 (2004) 131–142. doi:10.1007/s00253-004-1733-0.
- [2] UNEP, *Biodegradable Plastics and Marine Litter. Misconceptions, concerns and impacts on marine environments.*, United Nations Environment Programme (UNEP), Nairobi, 2015.
- [3] F. Liravi, E. Toyserkani, A hybrid additive manufacturing method for the fabrication of silicone bio-structures: 3D printing optimization and surface characterization, *Mater. Des.* 138 (2017) 46–61. doi:10.1016/j.matdes.2017.10.051.
- [4] B. Berman, 3-D printing: The new industrial revolution, *Bus. Horiz.* 55 (2012) 155–162. doi:10.1016/j.bushor.2011.11.003.
- [5] D. Ozdil, H.M. Aydin, Polymers for medical and tissue engineering applications, *J. Chem. Technol. Biotechnol.* 89 (2014) 1793–1810. doi:10.1002/jctb.4505.
- [6] H.N. Chia, B.M. Wu, Recent advances in 3D printing of biomaterials, *J. Biol. Eng.* 9 (2015) 1–14. doi:10.1186/s13036-015-0001-4.

- [7] L. Bedian, A.M. Villalba-Rodriguez, G. Hernandez-Vargas, R. Parra-Saldivar, H.M.N. Iqbal, Bio-based materials with novel characteristics for tissue engineering applications - A review, *Int. J. Biol. Macromol.* 98 (2017) 837–846. doi:10.1016/j.ijbiomac.2017.02.048.
- [8] R.S. Blackburn, *Sustainable Textiles: Life Cycle and Environmental Impact*, Woodhead Publishing, 2009.
- [9] T. Huber, J. Müssig, O. Curnow, S. Pang, S. Bickerton, M.P. Staiger, A critical review of all-cellulose composites, *J. Mater. Sci.* 47 (2012) 1171–1186. doi:10.1007/s10853-011-5774-3.
- [10] R. Melnikova, A. Ehrmann, K. Finsterbusch, 3D printing of textile-based structures by Fused Deposition Modelling (FDM) with different polymer materials, *IOP Conf. Ser. Mater. Sci. Eng.* 62 (2014). doi:10.1088/1757-899X/62/1/012018.
- [11] E. Pei, J. Shen, J. Watling, Direct 3D printing of polymers onto textiles: experimental studies and applications, *Rapid Prototyp. J.* 21 (2015) 556–571. doi:10.1108/RPJ-09-2014-0126.
- [12] L. Sabantina, F. Kinzel, A. Ehrmann, K. Finsterbusch, Combining 3D printed forms with textile structures - mechanical and geometrical properties of multi-material systems, *IOP Conf. Ser. Mater. Sci. Eng.* 87 (2015). doi:10.1088/1757-899X/87/1/012005.
- [13] R.H. Sanatgar, C. Campagne, V. Nierstrasz, Investigation of the adhesion properties of direct 3D printing of polymers and nanocomposites on textiles: Effect of FDM printing process parameters, *Appl. Surf. Sci.* 403 (2017) 551–563. doi:10.1016/j.apsusc.2017.01.112.
- [14] J.A. Lewis, J.E. Smay, J. Stuecker, J. Cesarano, Direct ink writing of three-dimensional ceramic structures, *J. Am. Ceram. Soc.* 89 (2006) 3599–3609. doi:10.1111/j.1551-2916.2006.01382.x.
- [15] M. Guvendiren, J. Molde, R.M.D. Soares, J. Kohn, Designing Biomaterials for 3D Printing, *ACS Biomater. Sci. Eng.* 2 (2016) 1679–1693. doi:10.1021/acsbiomaterials.6b00121.
- [16] D. Klemm, B. Philipp, T. Heinze, U. Heinze, W. Wagenknecht, *Comprehensive Cellulose Chemistry*, Wiley-VCH Verlag GmbH & Co. KGaA, Weinheim, FRG, 1998. doi:10.1002/3527601929.
- [17] A. van Wijk, I. van Wijk, 3D printing with biomaterials: Towards a sustainable and circular economy, 2015. doi:10.3233/978-1-61499-486-2-i.
- [18] K. Markstedt, A. Mantas, I. Tournier, H. Martínez Ávila, D. Hägg, P. Gatenholm, 3D Bioprinting Human Chondrocytes with Nanocellulose-Alginate Bioink for Cartilage Tissue Engineering Applications, *Biomacromolecules.* 16 (2015) 1489–1496. doi:10.1021/acs.biomac.5b00188.
- [19] K. Markstedt, J. Sundberg, P. Gatenholm, 3D Bioprinting of Cellulose Structures from an Ionic Liquid,

- 3D Print. Addit. Manuf. 1 (2014) 115–121. doi:10.1089/3dp.2014.0004.
- [20] S.W. Pattinson, A.J. Hart, Additive Manufacturing of Cellulosic Materials with Robust Mechanics and Antimicrobial Functionality, *Adv. Mater. Technol.* 2 (2017). doi:10.1002/admt.201600084.
- [21] K. Henke, S. Treml, Wood based bulk material in 3D printing processes for applications in construction, *Eur. J. Wood Wood Prod.* 71 (2013) 139–141. doi:10.1007/s00107-012-0658-z.
- [22] S.-L. Tseng, A. Valente, D.G. Gray, Cholesteric liquid crystalline phases based on (acetoxypopyl)cellulose, *Macromolecules.* 14 (1981) 715–719. doi:10.1021/ma50004a049.
- [23] G. V. Laivins, D.G. Gray, Characterization and chain stiffness of (Acetoxypopyl)cellulose, *Macromolecules.* 18 (1985) 1746–1752. doi:10.1021/ma00151a018.
- [24] R. Buchanan, Design Research and the New Learning, *Des. Issues.* 17 (2001) 3–23. doi:10.1162/07479360152681056.
- [25] H. Nowotny, P.B. Scott, M.T. Gibbons, *Re-Thinking Science: Knowledge and the Public in an Age of Uncertainty*, Cambridge: Polity, 2001.
- [26] C. Frayling, Research in Art and Design, *R. Coll. Art Res. Pap.* 1 (1993) 1–5. <http://www.opengrey.eu/handle/10068/492065>.
- [27] N. Cross, Designerly ways of knowing: design discipline versus design science, *Des. Issues.* 17 (2001) 49–55. doi:10.1162/074793601750357196.
- [28] F. Carrillo, X. Colom, J.J. Suñol, J. Saurina, Structural FTIR analysis and thermal characterisation of lyocell and viscose-type fibres, *Eur. Polym. J.* 40 (2004) 2229–2234. doi:10.1016/j.eurpolymj.2004.05.003.
- [29] C. Chung, M. Lee, E.K. Choe, Characterization of cotton fabric scouring by FT-IR ATR spectroscopy, *Carbohydr. Polym.* 58 (2004) 417–420. doi:10.1016/j.carbpol.2004.08.005.
- [30] M. Österberg, P.M. Claesson, Interactions between cellulose surfaces: effect of solution pH, *J. Adhes. Sci. Technol.* 14 (2000) 603–618. doi:10.1163/156856100742771.
- [31] M. Rodahl, B. Kasemo, A simple setup to simultaneously measure the resonant frequency and the absolute dissipation factor of a quartz crystal microbalance, *Rev. Sci. Instrum.* 67 (1996) 3238–3241. doi:10.1063/1.1147494.
- [32] F. Höök, M. Rodahl, P. Brezezinski, B. Kasemo, Energy Dissipation Kinetics for Protein and Antibody - Antigen Adsorption under Shear Oscillation on a Quartz Crystal Microbalance, *Langmuir.* 14 (1998) 729–734. doi:10.1021/la970815u.

- [33] G. Sauerbrey, The use of quartz oscillators for weighing thin layers and for microweighing, *Zeitschrift Für Phys.* 155 (1959) 206–222. doi:10.1007/BF01337937.
- [34] M. Rodahl, F. Höök, A. Krozer, P. Brzezinski, B. Kasemo, Quartz crystal microbalance setup for frequency and Q -factor measurements in gaseous and liquid environments, *Rev. Sci. Instrum.* 66 (1995) 3924–3930. doi:10.1063/1.1145396.
- [35] E. Kontturi, P.C. Thüne, J.W. Niemantsverdriet, Cellulose model surfaces-simplified preparation by spin coating and characterization by X-ray photoelectron spectroscopy, infrared spectroscopy, and atomic force microscopy, *Langmuir.* 19 (2003) 5735–5741. doi:10.1021/la0340394.
- [36] B. Kosan, C. Michels, F. Meister, Dissolution and forming of cellulose with ionic liquids, *Cellulose.* 15 (2008) 59–66. doi:10.1007/s10570-007-9160-x.
- [37] I. Rusig, M.H. Godinho, L. Varichon, P. Sixou, J. Dedier, C. Filliatre, A.F. Martins, Optical properties of cholesteric (2-hydroxypropyl) cellulose (HPC) esters, *J. Polym. Sci. Part B Polym. Phys.* 32 (1994) 1907–1914. doi:10.1002/polb.1994.090321108.
- [38] R. Kargl, T. Mohan, M. Bračč, M. Kulterer, A. Doliška, K. Stana-Kleinschek, V. Ribitsch, Adsorption of carboxymethyl cellulose on polymer surfaces: Evidence of a specific interaction with cellulose, *Langmuir.* 28 (2012) 11440–11447. doi:10.1021/la302110a.
- [39] P. Myllytie, J. Salmi, J. Laine, The Influence of pH on the Adsorption and Interaction of Chitosan with Cellulose, *BioResources.* 4 (2009) 1647–1662.
- [40] H. Orelma, T. Teerinen, L.S. Johansson, S. Holappa, J. Laine, CMC-modified cellulose biointerface for antibody conjugation, *Biomacromolecules.* 13 (2012) 1051–1058. doi:10.1021/bm201771m.
- [41] T. Tammelin, T. Saarinen, M. Österberg, J. Laine, Preparation of Langmuir/Blodgett-cellulose surfaces by using horizontal dipping procedure. Application for polyelectrolyte adsorption studies performed with QCM-D, *Cellulose.* 13 (2006) 519–535. doi:10.1007/s10570-005-9002-7.
- [42] E. Gustafsson, Tailoring adhesion and wetting properties of cellulose fibers and model surfaces, KTH Royal Institute of Technology, 2012.
- [43] S.L. Schaeffer, J. Slusarski, V. Vantiem, M.L. Johnson, Tensile Strength Comparison of Athletic Tapes : Assessed Using ASTM D3759M-96 , Standard Test Method for Tensile Strength and Elongation of Pressure-Sensitive Tapes, *J. Ind. Technol.* 16 (2000) 1–6.
- [44] D.H. Kaelble, Theory and Analysis of Peel Adhesion: Mechanisms and Mechanics, *Trans. Soc. Rheol.* 3 (1959) 161–180. doi:10.1122/1.548850.

- [45] M.D. Gower, R.A. Shanks, The effect of chain transfer agent level on adhesive performance and peel master-curves for acrylic pressure sensitive adhesives, *Macromol. Chem. Phys.* 205 (2004) 2139–2150. doi:10.1002/macp.200400177.
- [46] M. Ulbrich, J. Mühlsteff, A. Sipilä, M. Kamppi, A. Koskela, M. Myry, T. Wan, S. Leonhardt, M. Walter, The IMPACT shirt: textile integrated and portable impedance cardiography, *Physiol. Meas.* 35 (2014) 1181–1196. doi:10.1088/0967-3334/35/6/1181.
- [47] M. Faulde, G. Albiez, O. Nehring, Novel long-lasting impregnation technique transferred from clothing to bednets: Extended efficacy and residual activity of different pyrethroids against *Aedes aegypti* as shown by EN ISO 6330-standardized machine laundering, *Parasitol. Res.* 110 (2012) 2341–2350. doi:10.1007/s00436-011-2769-6.
- [48] M.L. Scarpello, I. Kazani, C. Hertleer, H. Rogier, D. Vande Ginste, Stability and efficiency of screen-printed wearable and washable antennas, *IEEE Antennas Wirel. Propag. Lett.* 11 (2012) 838–841. doi:10.1109/LAWP.2012.2207941.
- [49] V. Kumar, *101 Design Methods: A Structured Approach for Driving Innovation in Your Organization*, John Wiley & Sons, Inc, 2012.
- [50] D.A. Norman, R. Verganti, Incremental and Radical Innovation: Design Research vs. Technology and Meaning Change, *Des. Issues.* 30 (2014) 78–96. doi:10.1162/DESI\_a\_00250.
- [51] P.J. Stappers, Designing as a Part of Research, in: R.V.D. Lugt, P.J. Stappers (Eds.), *Des. Growth Knowl. Best Pract. Ingredients Success. Des. Res.*, Delft: ID Studiolar Press, 2006: pp. 12–17.
- [52] K.T. Ulrich, S.D. Eppinger, *Product Design and Development*, McGraw-Hill, 1995.
- [53] P.J. Stappers, Doing Design as a Part of Doing Research, in: R. Michel (Ed.), *Des. Res. Now*, Birkhäuser Basel, Basel, 2007: pp. 81–91. doi:10.1007/978-3-7643-8472-2\_6.
- [54] L. Li, M. Frey, Preparation and characterization of cellulose nitrate-acetate mixed ester fibers, *Polymer (Guildf).* 51 (2010) 3774–3783. doi:10.1016/j.polymer.2010.06.013.
- [55] B.J.C. Duchemin, A.P. Mathew, K. Oksman, All-cellulose composites by partial dissolution in the ionic liquid 1-butyl-3-methylimidazolium chloride, *Compos. Part A Appl. Sci. Manuf.* 40 (2009) 2031–2037. doi:10.1016/j.compositesa.2009.09.013.
- [56] M. Shibata, N. Teramoto, T. Nakamura, Y. Saitoh, All-cellulose and all-wood composites by partial dissolution of cotton fabric and wood in ionic liquid, *Carbohydr. Polym.* 98 (2013) 1532–1539. doi:10.1016/j.carbpol.2013.07.062.

- [57] M. Zavrel, D. Bross, M. Funke, J. Büchs, A.C. Spiess, High-throughput screening for ionic liquids dissolving (ligno-)cellulose, *Bioresour. Technol.* 100 (2009) 2580–2587. doi:10.1016/j.biortech.2008.11.052.
- [58] M. Isik, H. Sardon, D. Mecerreyes, Ionic Liquids and Cellulose: Dissolution, Chemical Modification and Preparation of New Cellulosic Materials, *Int. J. Mol. Sci.* 15 (2014) 11922–11940. doi:10.3390/ijms150711922.
- [59] C. Olsson, Cellulose processing in ionic liquid based solvents, Chalmers University of Technology, 2014.